Experimental investigation of hydronic snow melting process on the inclined pavement

Huajun Wang [a,*], Linbo Liu [a], Zhihao Chen [b]

[a] School of Energy and Environment Engineering, Hebei University of Technology, Tianjin 300401, China
[b] Faculty of Engineering, Yokohama National University, Yokohama, 240-8501, Japan

ARTICLE INFO

ABSTRACT

Hydronic snow melting on pavement has been used as an alternative to the conventional chemical method based on chloride salts. In the present work, dynamic snow-melting experiments were performed on a hydronically-heated inclined pavement. The effects of design parameters including the idling time, the fluid temperature and the tilt angle on the snow-melting time were analyzed. Further, the snow thickness profile during the snow-melting process was obtained. Experimental results showed that the symmetry of the snow-melting process around the hydronic pipes was destroyed on the inclined pavement, which is different from the case on the horizontal pavement. Because a part of melted slurry drained out of the snow-melting region, the capillary effect in the snow layer tended to be weakened, thereby prolonging the total snow-melting time. The phenomenon of critical free-area ratio was still found during the snow-melting process on the inclined pavement. The optimization of the layout of hydronic pipes and the idling time is a major approach to improving the performance of practical hydronic snow-melting systems.

© 2010 Elsevier B.V. All rights reserved.

1. Introduction

Traffic accidents occur frequently in many cold northern regions. It is desirable that ice and snow be removed effectively to keep normal traffic operations. At present, chemical salts have been applied extensively around the world. For instance, the annual amount of chemical deicing salts for snow melting in US has increased from one million tons in 1955 to 10 million tons in the late 1990s (Vitaliano, 1992; Godwin et al., 2003). In China, the annual amount of deicing salt is 100 thousand tons on average and seems to be increasing in recent years. However, deicing chemicals have obvious negative impacts including the concrete corrosion and environmental pollution (Ruth, 2003; Ramakrishna and Viraraghavan, 2005; Sanzo and Hecnar, 2006). This problem has been paid much attention.

Hydronic snow melting on pavement has been used as an alternative to the conventional chemical method. It has a remarkable advantage in using a low temperature heat sources including geothermal tail water, solar energy, and industrial waste heat. It is of great significance to energy saving and avoiding of additional CO_2 emissions. At present, several snow-melting systems have been applied in Japan, America, Iceland and other countries (Kinya and Shigeyuki, 2000; Rees and Spitler, 2002).

In previous theoretical studies, some steady-state algorithms for calculating the snow-melting load were presented by Chapman (1952), and then improved by Schnurr and Rogers (1970), Kilkis (1994a,b), and Ramsey (1999). These simplified algorithms were useful for the preliminary design of hydronic snow-melting systems. However, the dynamic snow-melting process was seldom taken into account. Recently, Wang et al. (2008) observed an interesting phenomenon on the critical free-area ratio (CFR), through a series of dynamic snow-melting experiments on the horizontal pavement. According to his experimental results, the snow-melting process tended to be accelerating once the snow free-area ratio on pavement exceeded the value of 0.6. This phenomenon was also found in Liu's similar experiments at Oklahoma University (Liu et al., 2007). Further, it was found that the capillary effect in the porous snow layer plays an important role in the complex heat and mass transfer from the pavement to the ambient. Such an explanation has been validated by both the experimental and numerical results (Wang and Chen, 2009).

All the above efforts mainly aimed at the horizontal pavement, in which the direction of the capillary force in snow is often treated by simplification as the opposite of gravity (Coleou et al., 1999; Jordan et al., 1999). However, practical snow-melting systems are mostly applied for the inclined pavements or bridges where the transportation safety tends to be worse in winter. For instance, the hydronic snow-melting system in Klamath Falls, Oregon was installed on the pavement with a tilt angle of about 8° (Lund, 1999). By far, it is still seldom studied on whether and how such a difference in the tilt angle of pavement has an impact on the snow-melting process. On the other hand, as Hockersmith indicated (2002), the amount of runoff flow on the horizontal pavement was usually limited to 10% of the melted rate of snow slurry. However, this amount tends to be greater on the

* Corresponding author. Tel./fax: +86 22 60204525.
  E-mail address: huajunwang@126.com (H. Wang).

inclined pavement, thereby influencing the capillary movement in the snow layer. With the background above, the main purpose of the present work is to analyze the effects of some major design parameters on the snow-melting time, and the effects of both the capillary effect and the runoff flow on the snow-melting process under the inclined pavement conditions, which can provide useful guides for the optimal design and energy-saving operation of practical hydronic snow-melting systems.

2. Experimental investigations

2.1. Experimental system

Fig. 1 shows a schematic diagram of the experimental setup of hydronic snow melting on pavement. The setup mainly consisted of a concrete pavement, a water heater, a circulation pump, a data acquisition system and hydronic pipes. The experimental pavement was poured with a mixture of cement and medium-coarse sand, and the mixing ratio of ingredients was approximately 1:2. The pavement was 500 mm in length, 400 mm in width and 300 mm in depth, and enclosed by woody plates with the thickness of 15 mm. After mixing and curing for a week, the concrete pavement was exposed to the ambient for natural drying. Three copper pipes with a diameter of 16 mm were used as hydronic pipes and embedded at a depth of 100 mm. The pipe spacing was 150 mm. All exposed pipes were connected by hose pipes and insulated effectively using rubber–plastic materials in order to reduce the undesired heat loss.

A Julabo PS-2 type constant-temperature water bath with ±0.2 °C accuracy was used to provide a low temperature heat source for snow melting. In this work, the temperature through the hydronic pipes ranged from 35 °C to 40 °C, which was very close to that of tail water from geothermal applications. The inlet and outlet fluid temperature through the hydronic pipes, together with the ambient temperature, were measured by Pt1000 sensors with ±0.1 °C accuracy. The mass flow rate through the hydronic pipes was measured and adjusted by a float type flow meter. The ambient wind speed was measured by a DEM6 type three cup anemometer with the maximum range of 30 m/s and ±0.2 m/s accuracy.

2.2. Experimental object and data treatment

In the present work, natural snow was used as an experimental object to be melted. After measurement, the density and the porosity of natural snow were 254 kg/m³ and 72.3% on average, respectively. This density was in agreement with the results reported by Yen (1991), in which the density of natural snow ranged from 100 to 300 kg/m³, depending on the meteorological conditions. In addition, according to the International Classification for Seasonal Snow on the Ground by IASH (Colbeck, 1982, 1986), the type of deposited snow in this experiment was determined as dry snow. It usually occurs when

the ambient temperature is below 0 °C, and disaggregated snow grains have little tendency to adhere to each other when pressed together. In this state, liquid water content approaches to zero and grain size usually ranges from 0.2 to 0.5 mm, which is also called as fine snow. During this experiment, the ambient temperature and wind speed ranged from −12 to −8 °C and from 1 to 2 m/s, respectively.

Fig. 2 shows a sectional view of snow-melting regions on the inclined pavement. For the convenience of comparative analysis, four snow-melting regions (i.e. A, B, C and D) and five position points (i.e. P1, P2, P3, P4 and P5) were marked. Considering the actual situation of most roads and bridges, the tilt angle of the experimental pavement was adjusted as 9° and 18°, respectively. In fact, the latter is almost close to the limit of climbing capacity of common cars. For most urban highways in China, the allowable tilt angle is lower than 9°.

For the design of hydronic snow-melting systems, the rate at which heat and mass transfer occur mainly depends on whether or not there is snow layer on pavement. Here, a dimensionless free-area ratio (FR) is defined as

$$FR = 1 - \frac{A_s}{A_t} \tag{1}$$

where A_s is the snow-covered area, and A_t is the total snow-melting area. Free-area ratio is a key design parameter for hydronic snow-melting systems, varying with different snow-melting requirements or classifications. Chapman (1952) early discussed the relationship between the snow-melting classifications and the free-area ratio aiming at residential, commercial and industrial applications. It has been recommended by ASHRAE (1998) as a technical guide. When the free-area ratio equals zero, the pavement is covered with snow to a certain depth. When the free-area ratio equals one, snow is melted rapidly enough that no accumulation occurs. Practical snow-melting systems usually operate somewhere between these limits. This is discussed in greater detail in a later section.

In this experiment, the dynamic snow-melting process within marked regions was observed and captured by a digital camera above the pavement. Then, the digital images were treated by the software MATLAB, and finally the free-area ratio was calculated by the ratio of the number of image pixels within the snow-free areas to the total pixel number. More details about the data treatment method were described in our previous study (Wang et al., 2008). The maximum error during treatment was determined as ±2%.

The snow-melting velocity, v, is defined as

$$v = \frac{m}{T} \tag{2}$$

where m is the mass of melted snow, and T is the melting time recorded at the moment when the heating starts. As Kilkis indicated (1994), the temperature profile on pavement is not uniform. Especially when the spacing between hydronic pipes is wide, the minimum surface temperature midway between adjacent hydronic pipes may drop below 0 °C, thereby resulting in ice formation on pavement. In this case, the pavement is necessary to be kept as a pre-heating or idling status in order to guarantee that the minimum
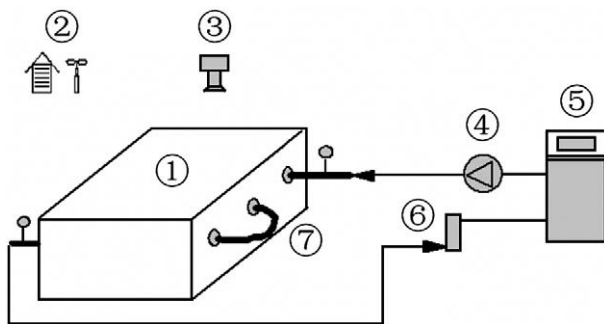

Fig. 1. Schematic diagram of the experimental setup of hydronic snow melting on pavement. 1. Concrete pavement; 2. ambient monitoring apparatus; 3. digital camera; 4. circulation pump; 5. water heater; 6. flow meter; and 7. hydronic pipes.
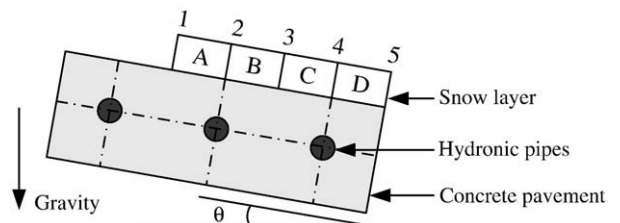

Fig. 2. Sectional view of snow-melting regions on the inclined pavement with hydronic pipes.

surface temperature is higher than 0 °C or 0.33 °C. The latter is recommended by ASHRAE (1998). For the idling process, T is recorded at the moment when snow is placed on pavement. Generally, a longer idling time is applied for the situation with a higher requirement for snow-melting.

3. Results and discussion

3.1. Effect of the idling time on the snow-melting process

Fig. 3 shows the variation of the free-area ratio during the snow-melting process in region B with and without the idling. Initial experimental conditions were as follows: (i) the tilt angle 9°, (ii) the heating fluid temperature 39.8 °C, and (iii) the average pavement temperature −2 °C, (iv) the snow thickness 27 mm. For the non-idling snow-melting process, the pavement temperature increased slowly after heating. This indicated that the surface-heating flux on pavement was too low to meet the requirement of immediate melting, thereby resulting in a delay on the melting time. The free-area ratio began to be greater than zero after 105 min and reached 1.0 at 136 min, with an average snow-melting velocity of 0.33 g/min. This period was too long for practical snow-melting applications. For the idling process, by contrast, the bare pavement surface appeared after 35 min due to a high snow-melting velocity of 1.0 g/min, and the total melting time was reduced by 68 min or 50%. Therefore, the idling time is a crucial factor to determine the performance of snow-melting systems. With respect to the above recommendation by ASHRAE, it is merely the lowest heating requirement. Wang (2007) presented a theoretical method to determine the idling time as the function of the layout of hydronic pipes, snow-melting requirements and ambient conditions. Usually, the melting time is reduced as the idling time is prolonged. On the other hand, it should be noted that a longer idling time also means higher energy consumptions for heating.

3.2. Effect of the fluid temperature on the snow-melting process

Fig. 4 shows the variation of the free-area ratio during the snow-melting process in region B with different fluid temperatures. Initial experimental conditions were the same as those in Fig. 3. It can be seen that the total snow-melting time is prolonged as the heating fluid temperature decreases. For instance, the snow-melting time was prolonged by 13.1%, when the fluid temperature decreased from 39.8 to 34.8 °C. This result was similar to that recently reported on horizontal pavements (Wang et al., 2008). Further, compared with the idling time, the effect of the fluid temperature on the snow-melting process is weaker. Therefore, a higher fluid temperature is unnecessary for the operation of hydronic snow-melting systems. This is favorable for applying a wider range of low-temperature heat sources. For instance, in Reykjavik, spent water (about 35 °C) from space heating of houses was commonly used for snow melting of sidewalks
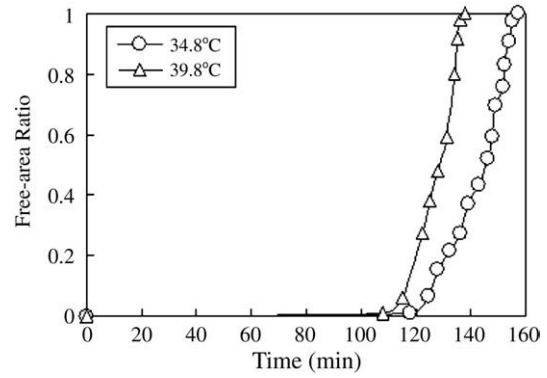

Fig. 4. Comparison of the snow free-area ratio under different fluid temperatures.

and parking spaces (Arni, 2005). In fact, if hydronic pipes are embedded properly, the temperature of ground water is sufficiently possible to melt the snow on pavement. Another similar case can be seen in the study by Nakamura (Nakamura et al., 1996). Generally, a high fluid temperature means much energy consumption. If the fluid temperature is too low, however, heat pump technologies are often used to improve the inlet fluid temperature through the hydronic pipes. For such a design, the total energy efficiency should be fully reevaluated, considering that extra electricity is consumed to driven the heat pump unit (Ogihara, 2005; Zhao and Wang, 2006).

3.3. Effect of the tilt angle on the snow-melting process

Fig. 5 shows the variation of the free-area ratio during the snow-melting process in region B with different tilt angles. Initial experimental conditions were the same as those in Fig. 3. It can be seen that, as the tilt angle increases, the snow-melting time is prolonged. Compared the horizontal pavement, the total snow-melting time at the tilt angle of 9° and 18° was increased by 25.9% and 53.7%, respectively. These results were obtained under the idling condition where the average pavement temperature had increased to 11.2 °C by preheating. For the situation without idling, the above difference in the snow-melting time may be greater. In spite of this, for most practical urban highways with the tilt angle of lower than 9°, the effect of the tilt angle on the snow-melting time can be controlled by idling to an acceptable range.

From the above results of comparative experiments, the phenomenon of CFR was still observed, but appeared weaker than that in our previous experiments on the horizontal pavement (Wang et al., 2008; Wang and Chen, 2009). This can be explained by two main reasons: (i) the temperature profile on pavement was improved by the smaller pipe spacing and the use of copper hydronic pipes instead of high-density polyethylene pipes (HDPEs); and (ii) the mechanism of the capillary effect was changed greatly under the inclined pavement
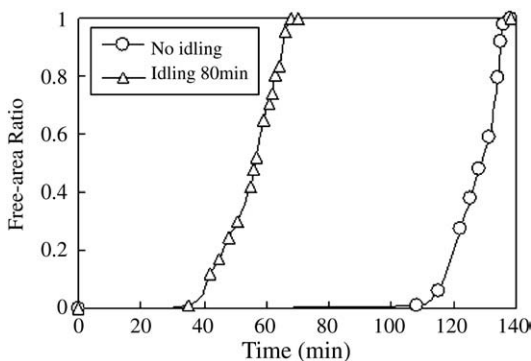

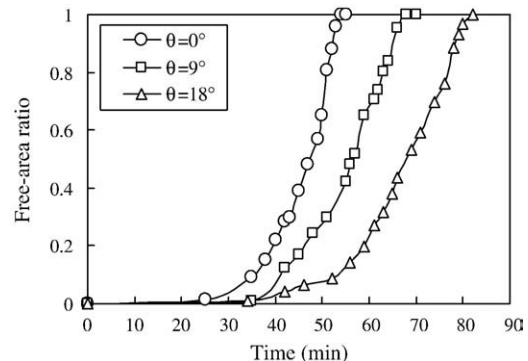Fig. 3. Comparison of the snow free-area ratio with and without the idling.

Fig. 5. Comparison of the snow free-area ratio under different tilt angles.
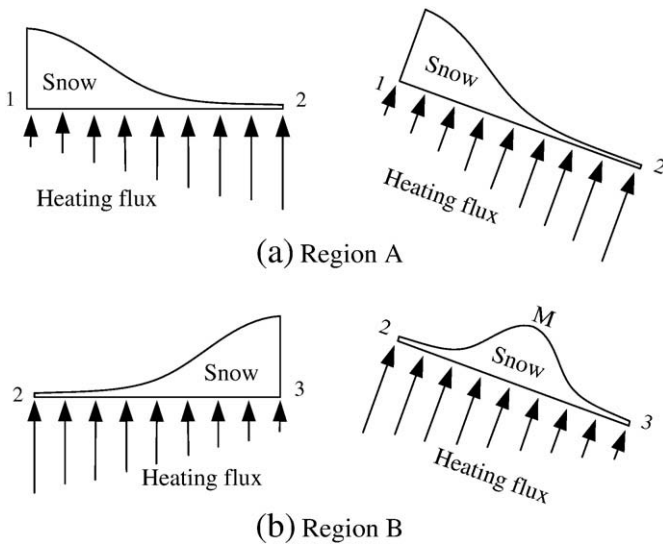
Fig. 6. Comparison of the snow-melting process on the horizontal and inclined pavement.

conditions, which is discussed in greater detail in the following section.

3.4. Analysis of the snow-melting characteristics on the inclined pavement

Previous studies showed that there is an axial symmetry of the snow-melting process around hydronic-heating pipes on the horizontal pavement. For the inclined pavement, however, this symmetry may be destroyed. Fig. 6 shows the snow thickness profile on both the horizontal and inclined pavement. For region A and B on the horizontal pavement, the snow-melting process proceeds simultaneously and symmetrically from P2 to P1 and from P2 to P3, respectively. For region A on the inclined pavement, the snow-melting process still proceeds from P2 to P1. For region B on the inclined pavement, however, there exists a new position point M between P2 and P3, and the snow-melting process proceeds basically from P2 to M and from P3 to M. Such an interesting phenomenon in region B reflects the influence of both the capillary action and the runoff flow on the hydronic snow-melting process on the inclined pavement. Its mechanism can be explained as follows.

Fig. 7 shows the variation of both the snow thickness and the free-area ratio in region B. Initial experimental conditions were the same as those in Fig. 3. At the initial stage of snow melting, heat conduction from hydronic pipes was dominated between the pavement and the snow layer. Due to the non-uniform temperature profile on pavement,
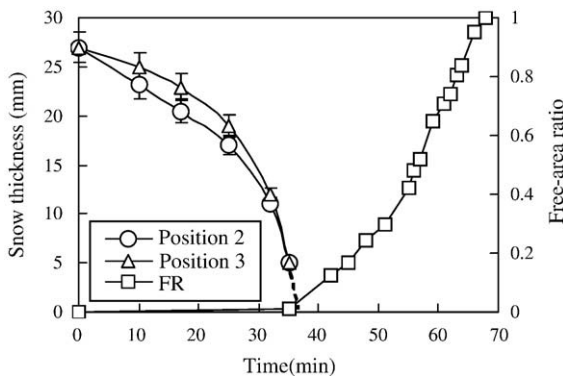

Fig. 7. Variation of the snow thickness and free-area ratio in region B.

which was determined by the layout of hydronic pipes, snow melted faster at P2 than at P3, as seen in the variation of the snow thickness during the first 35 min. However, as the melted snow slurry flowed downwards along the inclined pavement, the capillary effect was weakened at P2, but enhanced at P3. Thus, the snow melting at P3 began to accelerate, in spite of a lower surface-heating flux from hydronic pipes. The snow thickness at P2 and P3 reached the same level at 35 min, and dropped to zero at 37 min. This indicated that the bare pavement surface began to appear, with the free-area ratio of greater than zero. As the capillary process at P3 tended to be saturated gradually, except a part of melted slurry flowing out of the snow-melting region, the rest began to move towards P2 driven by the upward capillary effect. This phenomenon was reflected clearly by the movement of the wetting front.

Fig. 8 shows the dynamic snow-melting process in region B. From the photograph at 25 min, 37 min and 45 min, we can observe the movement of the wetting front during the snow-melting process. At this stage, the thermo-capillary convection governed the whole snow-melting process. Fig. 9 further shows a typical photograph of the snow thickness profile and the wetting front on the inclined pavement. In this experiment, the position of M was approximately located at the middle of P2 and P3. In fact, the accurate position of M depends mainly on the layout of hydronic pipes and the tilt angle of pavement, which will be reported in the future work. The snow layer became completely saturated at about 50 min, and the corresponding free-area ratio was about 0.24. From then on, the heat and mass transfer between the saturated snow layer and the ambient, including surface evaporation, convective cooling and external radiation, became completely dominated, instead of the capillary effect.

Fig. 10 compares the variation of the free-area ratio in different snow-melting regions without idling. It can be found again that the symmetry of the snow-melting process around the hydronic pipes on the inclined pavement was destroyed. From region A to region D, the snow-melting time tended to be increasing gradually. Especially, the snow layer in region D melted rapidly at the initial stage, due to a strong capillary effect caused by the convergence of the runoff, while the snow layer in region A melted slowly, due to a weak capillary effect and a lagging surface-heating flux on pavement. At the later stages, however, the snow-melting process in region D became slower, due to a strong cooling effect on the edge of the pavement, while the snow-melting process in region A became faster, due to a higher pavement temperature. In summary, compared with the horizontal pavement, because a part of melted slurry drained out of the snow-melting region, the capillary effect in the snow layer tended to be weakened, which finally prolonged the total snow-melting time. Therefore, for the design of hydronic snow-melting systems on the inclined pavement, it is recommended that a smaller spacing of hydronic pipes should be considered.

From the experimental results above, it can also be found that the time period of the free-area ratio ranging from 0.6 to 1 occupies only a smaller percentage to the total snow-melting time. This percentage was about 4–7% for the non-idling conditions, which was much lower than our previous experimental result of 28–32% (Liu et al., 2007; Wang et al., 2008). This was caused mainly by the difference in the material and layout of hydronic pipes. For the present experiments, copper pipes with a spacing of 150 mm were used, while for the previous studies, HDPEs with a spacing of 200 mm were used. In short, the above percentage has a decreasing tendency with the improvement on the uniformity of the pavement temperature profile. In addition, it was also observed that the snow thickness near the CFR of 0.6 was lower than 1 mm. Thus, even if the heating stops, the residual snow can be melted by heat energy stored in pavement. Therefore, in order to reduce the heating energy consumption, it is recommended that the free-area ratio should be kept as a value of around 0.6 for the design of hydronic snow-melting systems. For both the horizontal and inclined pavement, the optimization of the layout of hydronic pipes
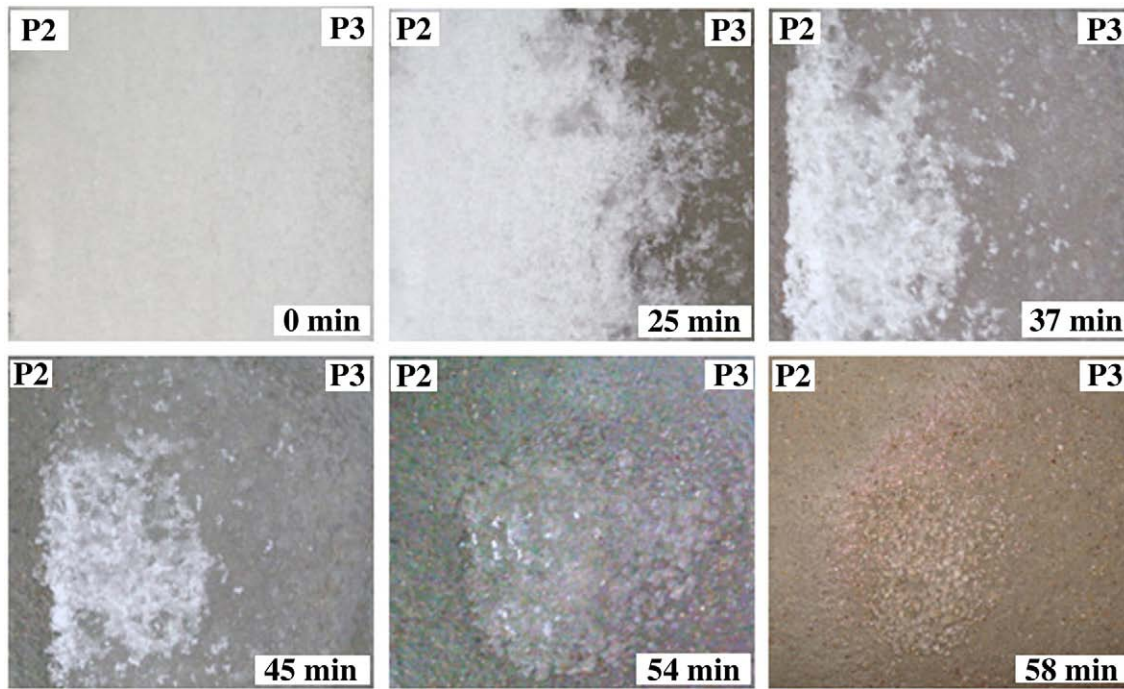
Fig. 8. Dynamic photograph of the snow-melting process in region B.

and the idling time is a major approach to improving the energy-saving performance of practical hydronic snow-melting systems.

4. Conclusions

Hydronic snow melting has a promising future as an alternative to the conventional chemical method. Based on our previous studies, a series of dynamic snow-melting experiments on a hydronically-heated inclined pavement were performed in the present work. From the experimental results discussed above, the following conclusions can be obtained:

(i) The idling time is a crucial factor to determine the operation performance of hydronic snow-melting systems. Compared the idling time, the effect of the fluid temperature on the snow-melting process is weaker. A high fluid temperature is unnecessary for the operation of hydronic snow-melting systems. In

addition, the effect of the tilt angle on the snow-melting time can be controlled by idling to an acceptable range for most practical urban highways.

(ii) For the inclined pavement, the symmetry of the snow-melting process around hydronic pipes is destroyed, which is different from the horizontal pavement. Because a part of melted slurry drained out of the snow-melting region, the capillary effect in the snow layer tended to be weakened, thereby prolonging the final snow-melting time. For the design of practical hydronic snow-melting systems on the inclined pavement, it is recommended that a smaller spacing of heating pipes should be considered to improve the uniformity of the pavement temperature profile.

(iii) The phenomenon of CFR still exists during the snow-melting process on the inclined pavement. For practical hydronic snow-melting systems, it is recommended that the free-area ratio should be kept as a value of around 0.6. For both horizontal and inclined pavements, the optimization of the layout of hydronic pipes and the idling time is a major approach to improving the performance of hydronic snow-melting systems.
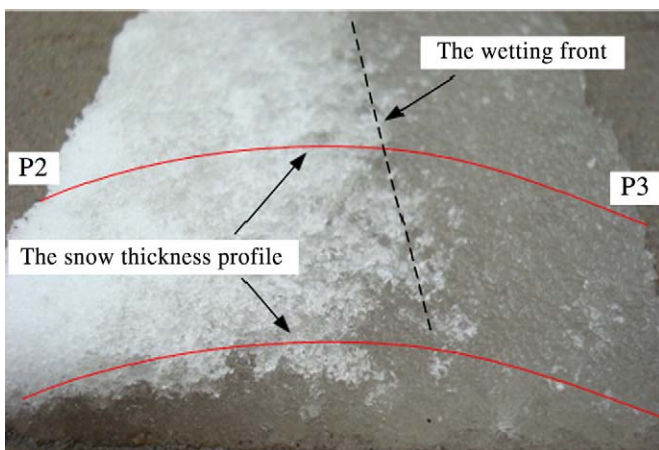

Fig. 9. Photograph of the snow thickness profile and the wetting front during the snow-melting process.
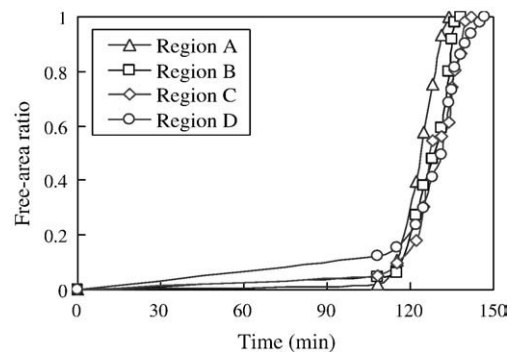

Fig. 10. Comparison of free-area ratio in different snow-melting regions.

Acknowledgements

References

Arni, R., 2005. Geothermal development in Iceland 2000–2004. Proceedings of World Geothermal Congress, Antalya, Turkey, pp. 11–16.

ASHRAE, 1998. ASHRAE handbook-fundamentals. American Society of Heating Refrigerating and Air-conditioning Engineers Inc, US, Atlanta.

Chapman, W.P., 1952. Design of snow melting systems. Heating and Ventilating 49 (4), 96–102.

Colbeck, S., 1982. An overview of seasonal snow metamorphism. Reviews of Geophysics and Space Physics 20 (1), 45–61.

Colbeck, S., 1986. Classification of seasonal snow cover crystals. Water Resources Research 22 (9), 59–70.

Coleou, C., Lesaffre, B., Brzoska, J., 1999. Capillary rise in snow. Hydrological Processes 13 (12–13), 1721–1732.

Godwin, A.S., Hafner, S.D., Buff, M.F., et al., 2003. Long-term trends in sodium and chloride in the Mohawk River, New York: the effect of fifty years of road-salt application. Environmental Pollution 124 (2), 273–281.

Hockersmith, S. L., 2000. Experimental and computational investigation of snow melting on heated horizontal surfaces. M.S.Thesis, Oklahoma State University, 2002.

Jordan, R.E., Hardy, J.P., Perron, F.E., et al., 1999. Air permeability and capillary rise as measures of the pore structure in snow: an experimental and theoretical study. Hydrological Processes 13 (12–13), 1733–1753.

Kilkis, I.B., 1994a. Design of embedded snow-melting systems.I: heat requirements — an overall assessment and recommendations. ASHRAE Transactions 100, 423–433.

Kilkis, I.B., 1994b. Design of embedded snow-melting systems. II: heat requirements – heat transfer in the slab – a simplified model. ASHRAE Transactions 100, 434–441.

Kinya, I., Shigeyuki, N., 2000. Prospects of snow melting systems using underground thermal energy storage in Japan. Proceedings of Annual Conference of the Society of Heating, Japan, pp. 154–160.

Liu, X., Rees, J., Spitler, S., 2007. Modeling snow melting on heated pavement surfaces. Part II: experimental validation. Applied Thermal Engineering 27 (10), 1125–1131.

Lund, J.W., 1999. Reconstruction of a pavement geothermal deicing system. Geo-Heat Center Quarterly Bulletin 20, 14–17.

Nakamura, H., Tanimoto, T., Hamada, S., 1996. Study of a snow-melting and antifreeze system for prevention of auto accidents on slippery bridge decks. Proceedings of International Conference on Snow Engineering, Sedan, Japan, pp. 439–442.

Ogihara, K., 2005. Heat pump system snow melt facility using underground heat: Hirosaki City sidewalk snow melt facility construction. MES/MSC Steel Construction Group Technical Review 18 (14), 116–118.

Ramakrishna, D.M., Viraraghavan, T.M., 2005. Environmental impact of chemical deicers — a review. Water, Air and Soil Pollution 166 (1–4), 49–63.

Ramsey, J.W., 1999. Updated design guideline for snow melting systems. ASHRAE Transactions 105, 1055–1065.

Rees, S.J., Spitler, J.D., 2002. Transient analysis of snow-melting system performance. ASHRAE Transactions 108, 406–423.

Ruth, O., 2003. The effects of de-icing in Helsinki urban streams, Southern Finland. Water Science and Technology 48 (9), 33–43.

Sanzo, D., Hecnar, S.J., 2006. Effect of road de-icing salt (NaCl) on larval wood frogs. Environmental Polution 140 (2), 247–256.

Schnurr, N.M., Rogers, D.B., 1970. Transient analysis of snow melting systems. ASHRAE Transactions 77 (2), 159–166.

Vitaliano, D., 1992. Economic assessment of the social costs of highway salting and the efficiency of substituting a new deicing material. Journal of Policy Analysis and Management 11 (3), 397–418.

Wang, H., 2007. Theoretical and experimental study of heat transfer of hydronic road snow-melting process. Ph.D.Thesis, Tianjin University.

Wang, H., Chen, Z., 2009. Study of critical free-area ratio during the snow-melting process on pavement using low-temperature heating fluids. Energy Conversion and Management 50 (1), 157–165.

Wang, H., Zhao, J., Chen, Z., 2008. Experimental investigation of ice and snow melting process on pavement utilizing geothermal tail water. Energy Conversion and Management 49 (6), 1538–1546.

Yen, Y., 1991. Review of intrinsic thermo-physical properties of snow, ice and sea ice. Northern Engineering 23 (1), 187–218.

Zhao, J., Wang, H., 2006. Seasonal behavior of pavement in geothermal snow-melting system with solar energy storage. Transactions of Tianjin University 12 (5), 319–324.